Fluctuations of conserved charges on the lattice and in heavy ion collisions



2014 J. Phys.: Conf. Ser. 535 012030

(http://iopscience.iop.org/1742-6596/535/1/012030)

Journal of Physics: Conference Series **535** (2014) 012030 doi:10.1088/1742-6596/535/1/012030

# Fluctuations of conserved charges on the lattice and in heavy ion collisions

**S. Borsanyi[1], Z. Fodor[1,2,3], S. D. Katz[2,4], S. Krieg[1,3], C. Ratti[5,6], K. K. Szabo[1,3]**

[1] Department of Physics, Wuppertal University, Gaussstr. 20, D-42119 Wuppertal, Germany
[2] Inst. for Theoretical Physics, Eötvös University, Pázmány P. sétány 1/A, H-1117 Budapest, Hungary
[3] Jülich Supercomputing Centre, Forschungszentrum Jülich, D-52425 Jülich, Germany
[4] MTA-ELTE "Lendület" Lattice Gauge Theory Research Group, Pázmány P. sétány 1/A, H-1117 Budapest, Hungary
[5] Dip. di Fisica, Università di Torino and INFN, Sezione di Torino via Giuria 1, I-10125 Torino, Italy
[6] Department of Physics, University of Houston, Houston, TX 77204, USA

E-mail: ratti@to.infn.it

**Abstract.** We present our latest results for fluctuations of electric charge and baryon number, simulated on the lattice in a system of 2+1 dynamical quark flavors at the physical quark masses and continuum extrapolated. In order to extract the chemical freeze-out temperature and chemical potential, we compare our results to the moments of multiplicity distribution of the corresponding conserved charges, measured in heavy ion collision experiments by the STAR collaboration. Consistency between the freeze-out parameters obtained through different conserved charges is discussed.

## 1. Introduction

Fluctuations of conserved charges have been the object of intense theoretical and experimental activity in the last few years. Several studies have identified fluctuations as ideal observables to spot the change from crossover to first-order phase transition in the QCD phase diagram [1, 2, 3]. Consequently the beam energy scan program at RHIC, in search for the QCD critical point, has recently published efficiency corrected results for these observables, in the collision-energy range $\sqrt{s} = 7.7 - 200$ GeV [4, 5]. Besides, it has been proposed to use fluctuations of conserved charges to extract the chemical freeze-out conditions of a heavy-ion collision from first principles, by comparing their experimental value to results of lattice QCD simulations at finite temperature and (small) chemical potential [6, 7, 8]. Such comparison assumes that, in the evolution of a heavy-ion collision, it is possible to identify two lines in the $(T, \mu_B)$ plane. The first one, called chemical freeze-out, is the point at which all inelastic interactions between particles cease: conserved charges are frozen at this time. The second one is the so-called kinetic freeze-out, at lower temperatures, at which all elastic interactions cease: the momentum of the particles is frozen at this time.

The chemical freeze-out has been extensively studied in the past, by means of a Statistical Hadronization Model (SHM) fit to the particle yields and ratios measured in experiments

[9, 10, 11, 12]. By decreasing the collision energy, the freeze-out chemical potential increases; repeating the analysis for a series of beam energies provides a freeze-out curve in the $(T, \mu)$ plane. Our lattice analysis relies on the same assumption as the SHM, namely that the experimentally measured fluctuations can be described in terms of a thermally equilibrated system. However, the advantage is a first principle determination of the freeze-out parameters, without having to rely on a model which can lead to different results when a different hadronic spectrum is included [13, 14].

In comparing lattice results to experimental ones, one has to make sure that possible sources of non-thermal fluctuations are kept under control. The data published by the STAR collaboration are corrected for several effects: the centrality-bin-width correction method minimizes effects due to volume variation because of finite centrality bin width; the finite reconstruction efficiency of the detector is corrected for, based on binomial probability distribution [15]; spallation protons, coming from the interaction with the beam-pipe, are removed by appropriate cuts in $p_T$ [5]. Effects due to kinematic cuts have been investigated in the Hadron Resonance Gas model and found to be small [16, 17]. Interactions in the hadronic phase and non-equilibrium effects might in principle affect fluctuations [18, 19]; the analysis that we are performing can be considered as a test for the validity of the equilibrium scenario: we are checking whether the freeze-out parameters yielded by different conserved charges (electric charge and baryon number) are consistent with each other. In particular, while the freeze-out temperature might be flavor-dependent [20], the chemical potentials as a function of the collision energy should be the same for all species. Therefore, in our approach we are able to check whether the three conserved charges $B, Q, S$ have a common freeze-out surface, or whether the chemical freeze-out is a more involved scenario which allows different surfaces for different conserved charges. The present level of precision reached by lattice QCD results, obtained at physical quark masses and continuum-extrapolated, allows to perform this check for the first time [21].

One more caveat in our analysis is worth mentioning: while lattice QCD can only address conserved charges, experimental fluctuations are limited to a sub-set of the full hadron spectrum; in particular, the net-proton multiplicity distribution is measured, as opposed to the lattice net-baryon number fluctuations. Recently it was shown that, once the effects of resonance feed-down and isospin randomization are taken into account [22, 23], the net-proton and net-baryon number fluctuations are numerically very similar [24].

In this manuscript we give an overview of the analysis that we performed in [21]: we systematically compare our continuum-extrapolated results on fluctuations of electric charge and baryon number to the most recent, efficiency corrected measurements by the STAR collaboration [4, 5]. This allows us to extract an upper limit for the chemical freeze-out temperature, as well as freeze-out chemical potentials for the four highest energies at RHIC. The independent analyses of electric charge and baryon number yield consistent results, thus validating our approach and the assumptions on which it is based.

## 2. Results

The definition of the fluctuations of baryon number, electric charge and strangeness is

$$\chi^{BSQ}_{lmn} = \frac{\partial^{l+m+n}(p/T^4)}{\partial(\mu_B/T)^l \partial(\mu_S/T)^m \partial(\mu_Q/T)^n}; \tag{1}$$

they are related to the moments of the multiplicity distributions of the corresponding conserved charges. The following, volume-independent ratios, are usually introduced, in order to get rid of the extra volume unknown parameter:

$$\begin{aligned} \chi_3/\chi_2 &= S\sigma \quad ; \quad \chi_4/\chi_2 = \kappa\sigma^2 \\ \chi_1/\chi_2 &= M/\sigma^2 \quad ; \quad \chi_3/\chi_1 = S\sigma^3/M\,. \end{aligned} \tag{2}$$

The chemical potentials $\mu_B$, $\mu_Q$ and $\mu_S$ are not independent: a relationship between them is obtained, in order to match the experimental situation. The finite baryon density in the system is due to light quarks only, since it is generated by the nucleon stopping in the collision region. The strangeness density $\langle n_S \rangle$ is then equal to zero for all collision energies, as a consequence of strangeness conservation. Besides, the electric charge and baryon-number densities are related, in order to match the isospin asymmetry of the colliding nuclei: $\langle n_Q \rangle = Z/A \langle n_B \rangle$. $Z/A = 0.4$ represents a good approximation for Pb-Pb and Au-Au collisions. As a consequence, $\mu_Q$ and $\mu_S$ depend on $\mu_B$ so that these conditions are satisfied. This is achieved by Taylor-expanding the densities in these three chemical potentials up to $\mu_B^3$ [7]:

$$\begin{aligned} \mu_Q(T,\mu_B) &= q_1(T)\mu_B + q_3(T)\mu_B^3 + ... \\ \mu_S(T,\mu_B) &= s_1(T)\mu_B + s_3(T)\mu_B^3 + ... \end{aligned} \tag{3}$$

Our continuum extrapolated results for the functions $q_1(T)$, $q_3(T)$, $s_1(T)$, $s_3(T)$ were shown in [8]. The quantities that we consider to extract the freeze-out $T$ and $\mu_B$, are the ratios $R_{31}^B = \chi_3^B/\chi_1^B$ and $R_{12}^B = \chi_1^B/\chi_2^B$ respectively, at values of $(\mu_B, \mu_Q, \mu_S)$, which satisfy the pyhsical conditions discussed in the previous paragraph.

The first terms of their Taylor expansion around $\mu_B = 0$ read:

$$\begin{aligned} R_{31}^B(T,\mu_B) &= \frac{\chi_3^B(T,\mu_B)}{\chi_1^B(T,\mu_B)} = \frac{\chi_4^B(T,0) + \chi_{31}^{BQ}(T,0)q_1(T) + \chi_{31}^{BS}(T,0)s_1(T)}{\chi_2^B(T,0) + \chi_{11}^{BQ}(T,0)q_1(T) + \chi_{11}^{BS}(T,0)s_1(T)} + \mathcal{O}(\mu_B^2) \\ R_{12}^B(T,\mu_B) &= \frac{\chi_1^B(T,\mu_B)}{\chi_2^B(T,\mu_B)} = \frac{\chi_2^B(T,0) + \chi_{11}^{BQ}(T,0)q_1(T) + \chi_{11}^{BS}(T,0)s_1(T)}{\chi_2^B(T,0)} \frac{\mu_B}{T} + \mathcal{O}(\mu_B^3). \end{aligned} \tag{4}$$

From the above equations, it is straightforward to identify $R_{31}^B$ as an ideal thermometer, since its leading order is independent of $\mu_B$. Once the freeze-out temperature has been extracted from $R_{31}^B$, it can then be plugged into $R_{12}^B$: the latter can then be used to extract the freeze-out chemical potential (notice that our results for $R_{12}^B$ are obtained up to NLO in $\mu_B$).

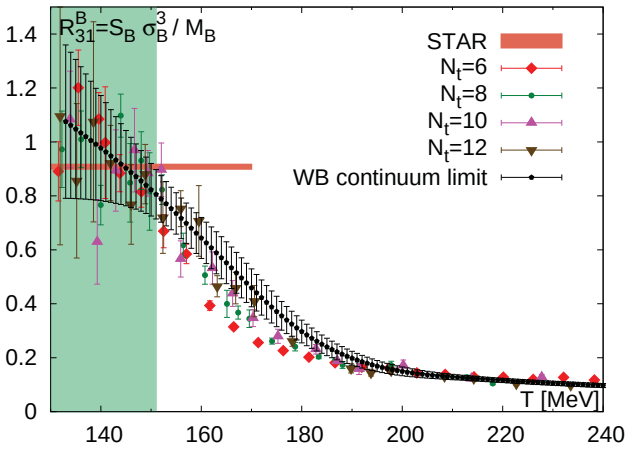


**Figure 1.** $R_{31}^B$: the colored symbols show finite-$N_t$ lattice QCD results. The continuum extrapolation is represented by black points (from Ref. [8]). The dark-orange band shows the recent experimental measurement by the STAR collaboration [4]: it was obtained by averaging the 0-5% and 5-10% data at the four highest energies ($\sqrt{s}$ = 27, 39, 62.4, 200 GeV). The green-shaded area shows the valid temperature range.

A similar expansion in $\mu_B$ holds also for the fluctuations of electric charge [8]: the leading order in $\chi_3^Q/\chi_1^Q$ is independent of $\mu_B$, while the LO in $\chi_2^Q/\chi_1^Q$ is linear in $\mu_B$. The present precision reached by the experimental results on $\chi_3^Q/\chi_1^Q$ does not allow an independent

determination of $T_f$. However, we are able to extract independent estimates of the freeze-out chemical potential from $R_{12}^B$ and $R_{12}^Q$.

In Fig. 1 we show the comparison between the lattice results for $\chi_3^B(T,\mu_B)/\chi_1^B(T,\mu_B)$ and the experimental measurement of $S_p\sigma_p^3/M_p$ by the STAR collaboration [4]. The latter is obtained by averaging the 0-5% and 5-10% centrality data, at the four highest energies ($\sqrt{s} = 27,\ 39,\ 62.4,\ 200$ GeV). Since the curvature of the phase diagram is small around $\mu_B = 0$ [25], it is safe to assume that this average allows to determine the freeze-out temperature for small $\mu_B$. The green-shaded area shows the valid temperature range: due to the uncertainty on the lattice results in the low-temperature regime, at the moment it is only possible to extract an upper value for the freeze-out temperature: the freeze-out takes place at a temperature $T_f \leq 151$ MeV, which is somewhat lower than expected from previous analyses based on preliminary, not efficiency corrected data [26] (allowing for a two-sigma deviation for the lattice simulations and the experimental measurements, the highest possible $T_f$ is 155 MeV). In Refs. [27, 28] we have published the lattice determination of the transition temperature from various chiral observables in the range 147-157 MeV. For the minimum of the speed of sound we found 145(5) MeV in [29]. The discussed freeze-out temperature is thus in the cross-over region around or slightly below the central value.

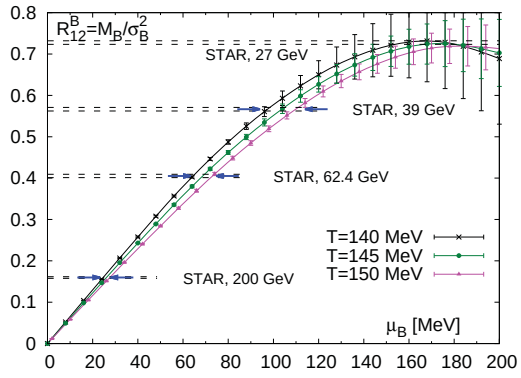


**Figure 2.** $R_{12}^B$ as a function of $\mu_B$. The three points correspond to the STAR data for $M_p/\sigma_p^2$ at collision energies $\sqrt{s} = 39,\ 62.4,\ 200$ GeV and centrality 0-10%, from Ref. [4] (the $\sqrt{s} = 27$ GeV point is also shown, but the non-monotonicity of the lattice results at $\mu_B \geq 130$ MeV does not allow a determination of $\mu_B$ from it). The arrows show the extracted values for $\mu_B$ at freeze-out.

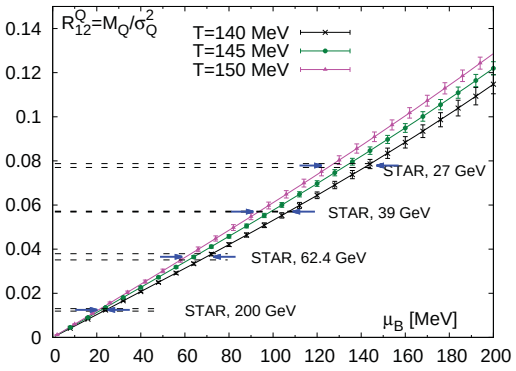


**Figure 3.** $R_{12}^Q$ as a function of $\mu_B$. The four points correspond to the STAR data for $M_Q/\sigma_Q^2$ at $\sqrt{s} = 27,\ 39,\ 62.4,\ 200$ GeV and centrality 0-10%, from Ref. [5]. In both figures, the colored symbols correspond to the lattice QCD results in the continuum limit, for the range ($140 \leq T_f \leq 150$) MeV. The arrows show the extracted values for $\mu_B$ at freeze-out.

We can now determine the freeze-out chemical potential $\mu_B$, by comparing the lattice results for $R_{12}^B$ as function of the chemical potential, and in the temperature range ($140 \leq T_f \leq 150$) MeV to the experimental results for $M_p/\sigma_p^2$ published by the STAR collaboration in Ref. [4, 30]. This procedure is shown in Fig. 2. In Fig. 3 we repeat the analysis for $R_{12}^Q$ vs $M_Q/\sigma_Q^2$ published by the STAR collaboration in Ref. [5]. The two quantities allow for an independent determination of $\mu_B$ from electric charge and baryon number: the corresponding values are listed in Table 1, and shown in Fig. 4. Consistency between the two values of baryon-chemical potential is found for all collision energies (notice that the non-monotonicity of the lattice results for $R_{12}^B$ at

$\mu_B \geq 130$ MeV does not allow a determination of $\mu_B$ from this observable at $\sqrt{s} = 27$ GeV). We also compare the chemical potentials in Table 1 to those found earlier in statistical fits [11, 9]: we find a remarkable agreement (see Fig. 4).

**Table 1.** Freeze-out $\mu_B$ vs. $\sqrt{s}$, for the four highest-energy STAR measurements. The $\mu_B$ values and error-bars in this table have been obtained under the assumption that 140 MeV $\leq T_f \leq$ 150 MeV. This uncertainty dominates the overall errors. Other (minor) sources of uncertainty are the lattice statistics and the experimental error.

| $\sqrt{s}[GeV]$ | $\mu_B^f$ [MeV] (from $B$) | $\mu_B^f$ [MeV] (from $Q$) |
|---|---|---|
| 200 | 25.8±2.7 | 22.8±2.6 |
| 62.4 | 69.7±6.4 | 66.6±7.9 |
| 39 | 105±11 | 101±10 |
| 27 | - | 136±13.8 |

Consistency between the two values of baryon-chemical potential is found for all collision energies (the non-monotonicity of the lattice results for $R_{12}^B$ at $\mu_B \geq 130$ MeV does not allow a determination of $\mu_B$ from this observable at $\sqrt{s} = 27$ GeV). We also compare the chemical potentials in Table 1 to those found earlier in statistical fits [11, 9]: we find a remarkable agreement (see Fig. 4).

Note that, in spite of the remarkable agreement between the chemical potentials obtained from the lattice and SHM analyses, for the freeze-out temperature statistical models typically yield a somewhat higher value: e.g. 164 MeV in Refs. [32, 9]. The latest fit to particle ratios from the ALICE collaboration [35] yields a temperature $T_{ch} \simeq 156$ MeV. However, it was pointed out that the protons are overestimated by this temperature: they would be optimally reproduced with a temperature consistent with the upper limit that we find in our analysis. Towards the lower end in temperature range we find also Ref. [33] with $T_f = 155 \pm 8$ MeV and $\mu_B = 25 \pm 1$ MeV, at $\sqrt{s} = 200$ GeV.

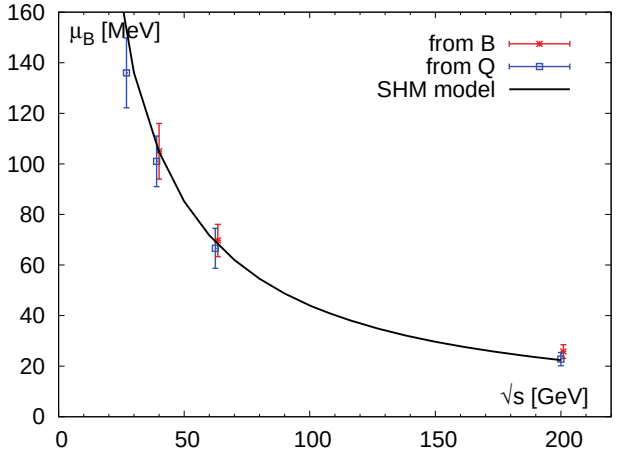


**Figure 4.** Freeze-out chemical potential $\mu_B$ as a function of the collision energy. The red stars show the $\mu_B$ obtained by fitting $R_{12}^B$, the blue squares have been obtained by fitting $R_{12}^Q$. The black curve comes from the Statistical Hadronization Model analysis of Refs. [9].

Our analysis finds a consistency between the freeze-out chemical potentials obtained from electric charge and baryon number, if we assume an agreement in the corresponding freeze-out temperatures. If the freeze-out can be described by the same temperature and chemical

potentials for charge and protons, then one can define a combined observable: $R_{12}^{Q}/R_{12}^{B} = [M_Q/\sigma_Q^2]/[M_B/\sigma_B^2]$. Here, the volume factor of the charge and baryon (proton) measurements cancel separately. This ratio of ratios is an ideal thermometer: it is far easier to obtain both for lattice and experiment since it does not involve skewness or kurtosis which are obviously affected by larger error bars; besides, the lattice curve shows a high sensitivity to the temperature, thus allowing a more precise determination of $T_f$. A comparison between lattice results and experimental measurement for this observable is shown in Fig. 5. Contrary to the skewness thermometer, here we see a clear monotonic temperature dependence without the hardly controllable lattice errors at low temperatures. This allows for the identification of a narrow temperature band, instead of an upper limit.

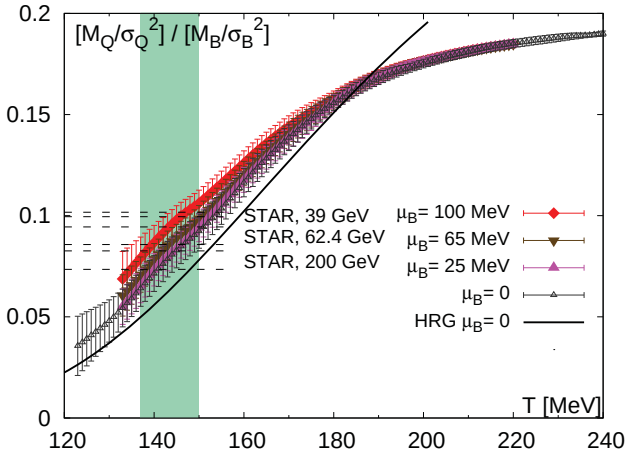


**Figure 5.** $R_{12}^{Q}/R_{12}^{B}$: the colored symbols correspond to continuum-extrapolated lattice QCD simulations at different values of $\mu_B$. The dashed lines shows the recent experimental measurements by the STAR collaboration [4, 5] for a 0-10% centrality and different collision energies. The green-shaded area shows the valid temperature range, $T_f = (144 \pm 6)$ MeV.

The thermometer in Fig. 5 represents also an important consistency criterion: it agrees to the experimental data in the temperature range which needs to be assumed to have a common chemical potential between electric charge and baryon number. For high enough energies ($\sqrt{s} \geq$ 39 GeV) this consistency is granted if freeze-out occurs in the range $T_f = 144 \pm 6$ MeV. Notice that this temperature range lies just below the upper limit that we determined independently in Fig. 1.

## 3. Conclusions

In the present paper we have extracted the freeze-out conditions of heavy-ion collisions (temperature and chemical potential) from first principles, by comparing our continuum extrapolated lattice QCD results to the experimental moments of net-charge and net-proton multiplicity distribution by the STAR collaboration. Due to the present uncertainty in the lattice data, as well as the difficulty of simulating at finite chemical potential, we were able to obtain an upper limit for the chemical freeze-out temperature, and freeze-out chemical potentials for the four highest collision energies at RHIC. These new, efficiency corrected, experimental data point at a lower freeze-out temperature compared to previous estimates. This is compatible with the expectation that the freeze-out should occur just below the transition. The freeze-out chemical potentials obtained from an independent analysis of electric charge and baryon number fluctuations show a remarkable consistency with each other, as well as with previous results from the Statistical Hadronization Model. This comparison is possible for the first time, and the consistency of the results is of fundamental importance to validate the hypothesis on which this method is based, namely that the experimentally created system is close to thermal equilibrium at the freeze-out and can be described by lattice QCD simulations, at least in the light quark sector.

**Acknowledgements**
C. Ratti acknowledges fruitful discussions with Francesco Becattini, Rene Bellwied and Bill Llope. This project was funded by the DFG grant SFB/TR55. The work of C. Ratti is supported by funds provided by the Italian Ministry of Education, Universities and Research under the Firb Research Grant RBFR0814TT. S. D. Katz is funded by the ERC grant ((FP7/2007-2013)/ERC No 208740) as well as the "Lendület" program of the Hungarian Academy of Sciences ((LP2012-44/2012). The numerical simulations were performed on the QPACE machine, the GPU cluster at the Wuppertal University and on JUQUEEN (the Blue Gene/Q system of the Forschungszentrum Juelich) and on MIRA at the Argonne Leadership Computing Facility through the Innovative and Novel Computational Impact on Theory and Experiment (INCITE) program of the U.S. Department of Energy (DOE).

**References**

[1] M. A. Stephanov, K. Rajagopal and E. V. Shuryak, Phys. Rev. D **60**, 114028 (1999)
[2] R. V. Gavai and S. Gupta, Phys. Rev. D **78**, 114503 (2008)
[3] M. Cheng, *et al.*, Phys. Rev. D **77**, 014511 (2008)
[4] L. Adamczyk *et al.* [STAR Collaboration], Phys. Rev. Lett. **112**, no. 3, 032302 (2014)
[5] L. Adamczyk *et al.* [STAR Collaboration], arXiv:1402.1558 [nucl-ex].
[6] F. Karsch, Central Eur. J. Phys. **10**, 1234 (2012)
[7] A. Bazavov, *et al.*, Phys. Rev. Lett. **109**, 192302 (2012)
[8] S. Borsanyi, Z. Fodor, S. D. Katz, S. Krieg, C. Ratti and K. K. Szabo, Phys. Rev. Lett. **111** (2013) 062005
[9] A. Andronic, P. Braun-Munzinger and J. Stachel, Phys. Lett. B **673** (2009) 142 [Erratum-ibid. B **678** (2009) 516]
[10] F. Becattini, J. Manninen and M. Gazdzicki, Phys. Rev. C **73**, 044905 (2006)
[11] J. Cleymans, H. Oeschler, K. Redlich and S. Wheaton, Phys. Rev. C **73** (2006) 034905
[12] J. Manninen and F. Becattini, Phys. Rev. C **78**, 054901 (2008)
[13] J. Noronha-Hostler and C. Greiner, arXiv:1405.7298 [nucl-th].
[14] A. Bazavov, H. -T. Ding, P. Hegde, O. Kaczmarek, F. Karsch, E. Laermann, Y. Maezawa and S. Mukherjee *et al.*, arXiv:1404.6511 [hep-lat].
[15] A. Bzdak and V. Koch, Phys. Rev. C **86** (2012) 044904
[16] P. Garg, D. K. Mishra, P. K. Netrakanti, B. Mohanty, A. K. Mohanty, B. K. Singh and N. Xu, Phys. Lett. B **726**, 691 (2013)
[17] P. Alba, W. Alberico, R. Bellwied, M. Bluhm, V. M. Sarti, M. Nahrgang and C. Ratti, arXiv:1403.4903 [hep-ph].
[18] J. Steinheimer, J. Aichelin and M. Bleicher, Phys. Rev. Lett. **110** (2013) 042501
[19] F. Becattini, M. Bleicher, T. Kollegger, T. Schuster, J. Steinheimer and R. Stock, Phys. Rev. Lett. **111** (2013) 082302
[20] R. Bellwied, S. Borsanyi, Z. Fodor, S. DKatz and C. Ratti, Phys. Rev. Lett. **111** (2013) 202302
[21] S. Borsanyi, Z. Fodor, S. D. Katz, S. Krieg, C. Ratti and K. K. Szabo, arXiv:1403.4576 [hep-lat].
[22] M. Kitazawa and M. Asakawa, Phys. Rev. C **85** (2012) 021901
[23] M. Kitazawa and M. Asakawa, Phys. Rev. C **86** (2012) 024904 [Erratum-ibid. C **86** (2012) 069902]
[24] M. Nahrgang, M. Bluhm, P. Alba, R. Bellwied and C. Ratti, arXiv:1402.1238 [hep-ph].
[25] G. Endrodi, Z. Fodor, S. D. Katz and K. K. Szabo, JHEP **1104**, 001 (2011)
[26] S. Mukherjee and M. Wagner, PoS CPOD **2013** (2013) 039
[27] Y. Aoki, S. Borsanyi, S. Durr, Z. Fodor, S. D. Katz, S. Krieg and K. K. Szabo, JHEP **0906** (2009) 088
[28] S. Borsanyi *et al.* [Wuppertal-Budapest Collaboration], JHEP **1009** (2010) 073
[29] S. Borsanyi, G. Endrodi, Z. Fodor, A. Jakovac, S. D. Katz, S. Krieg, C. Ratti and K. K. Szabo, JHEP **1011** (2010) 077
[30] The efficiency-corrected data for the lowest cumulant ratio $(c_2/c_1)$ for net-protons can be found on the public STAR webpage.
[31] A. Andronic, P. Braun-Munzinger and J. Stachel, Nucl. Phys. A **772** (2006) 167
[32] J. Adams *et al.* [STAR Collaboration], Nucl. Phys. A **757** (2005) 102
[33] J. Rafelski, J. Letessier and G. Torrieri, Phys. Rev. C **72** (2005) 024905
[34] P. Braun-Munzinger, J. Stachel and C. Wetterich, Phys. Lett. B **596** (2004) 61
[35] M. Floris, Proceedings of Quark Matter 2014, to appear in Nucl. Phys. A.